Published in final edited form as:
Neuron. 2010 January 14; 65(1): 32. doi:10.1016/j.neuron.2009.12.001.

Genetically increased cell-intrinsic excitability enhances neuronal integration into adult brain circuits

Chia-Wei Lin, **Shuyin Sim**, **Alice Ainsworth**, **Masayoshi Okada**, **Wolfgang Kelsch**, and **Carlos Lois**

Abstract

New neurons are added to the adult brain throughout life, but only half ultimately integrate into existing circuits. Sensory experience is an important regulator of the selection of new neurons but it remains unknown whether experience provides specific patterns of synaptic input, or simply a minimum level of overall membrane depolarization critical for integration. To investigate this issue, we genetically modified intrinsic electrical properties of adult-generated neurons in the mammalian olfactory bulb. First, we observed that suppressing levels of cell-intrinsic neuronal activity via expression of ESKir2.1 potassium channels decreases, whereas enhancing activity via expression of NaChBac sodium channels increases survival of new neurons. Neither of these modulations affects synaptic formation. Furthermore, even when neurons are induced to fire dramatically altered patterns of action potentials, increased levels of cell-intrinsic activity completely blocks cell death triggered by NMDA receptor deletion. These findings demonstrate that overall levels of cell-intrinsic activity govern survival of new neurons and precise firing patterns are not essential for neuronal integration into existing brain circuits.

A striking feature of nervous system development is that many more neurons are produced than are ultimately retained in the mature nervous system (Buss et al., 2006). Neuronal addition persists throughout life in the dentate gyrus of the hippocampus and the olfactory bulb (OB), where there continues to be overproduction and subsequent selection of neurons (Petreanu and Alvarez-Buylla, 2002; Winner et al., 2002; Yamaguchi and Mori, 2005). Unlike during embryonic development, neurons born postnatally are added to functionally mature circuits where their integration is believed to be regulated by sensory input or the behavioral state of the animal (Kee et al., 2007; Petreanu and Alvarez-Buylla, 2002).

It is postulated that the addition of new neurons into the adult brain may be a mechanism for lifelong learning and behavioral adaptation (Aimone et al., 2006; Lledo et al., 2006). Since only half of adult-generated neurons ultimately survive and integrate, it has been hypothesized that only new neurons that form relevant connections are incorporated to achieve fine-tuning of existing neuronal circuits (Aimone et al., 2006; Alonso et al., 2006; Kee et al., 2007; Lledo et al., 2006; Mouret et al., 2008; Wilbrecht et al., 2002). From experiments involving sensory deprivation in the OB and ablation of the NMDA receptor in the dentate gyrus, it is clear that synaptic input is a key regulator of the integration of adult-born neurons (Alonso et al., 2006; Kee et al., 2007; Mouret et al., 2008; Tashiro et al., 2006a; Wilbrecht et al., 2002). This idea is further supported by studies showing a preferential incorporation of adult-generated neurons into active circuits in the dentate gyrus (Kee et al., 2007). In addition, we have recently

demonstrated that olfactory deprivation perturbs synaptic development of new neurons in the adult OB and that genetically increasing the intrinsic excitability of individual neurons blocks the changes in synaptic density triggered by sensory deprivation (Kelsch et al., 2009). These observations suggest an interaction between sensory input and intrinsic neuronal activity in synapse formation, and possibly neuronal survival. However, it is still unclear whether the contribution of synaptic input is mainly to provide a precise pattern of neuronal activity to the new neurons, or merely a minimum level of membrane depolarization necessary for their selection and integration.

The elucidation of the mechanisms regulating the integration of new neurons has important implications both for understanding how neural circuits are constructed, as well as for successful implementation of stem cell-based replacement therapies for brain repair and neurodegenerative diseases. To evaluate the effect of suppressing or elevating electrical activity on the integration of young neurons into the OB, we used retroviral vectors to introduce ion channels into neuronal progenitors in the brains of adult rodents. In the current study, we found that overall levels of activity within a new neuron determined its integration into the circuit irrespective of firing patterns. Moreover, increasing intrinsic activity was sufficient to partially overcome cell death induced by sensory deprivation, and completely rescued neurons deficient in the NMDA receptor. Our observations reveal a rule of neuronal integration that is reliant on overall levels of membrane depolarization rather than on a specific pattern of firing.

RESULTS

Expression of the potassium channel ESKir2.1 dampens electrical activity in adult-generated neurons

The vast majority of new neurons in the OB of adult mammals are granule cells (GCs), inhibitory neurons whose progenitors reside in the subventricular zone (SVZ) (Lois and Alvarez-Buylla, 1994). Neuroblasts generated in the SVZ move along the rostral migratory stream toward the core of the OB and subsequently migrate radially into the granule cell layers. We genetically labeled adult born GCs by injecting retroviral vectors into the SVZ of adult rats. Since retroviral vectors only infect dividing cells, the progenitor cells within the SVZ are labeled but not mature neurons. We later monitored the subsequent integration of new GCs into the OB. The first arriving neuroblasts appeared in the adult rat OB as early as at 5 dpi. By 21 dpi, migrating neuroblasts still in the RMS contributed to 7.4% of the cells in the OB. By 28 dpi, the late arriving neuroblasts contributed to less than 2 percent of total infected cells inside the OB. The low infectivity rate of the retroviruses *in vivo* results in the modification of a very small proportion of GCs (less than 0.01% of all GCs), which appear randomly distributed throughout the bulb, thus negligibly perturbing the rest of the circuit (Kelsch et al., 2008; Kelsch et al., 2007).

To accurately assess neuronal integration, we injected approximate 1:1 titers of mixtures of a virus encoding the channel under study (tagged by GFP) and a virus encoding mCherry, so that mCherry-expressing neurons could be used as age-matched controls. We divided the number of GFP^+ and doubly infected (GFP^+ and $mCherry^+$) neurons by the number of $mCherry^+$-only neurons to derive a survival ratio and used the raw 7 dpi ratio to normalize subsequent time points. Thus, the 7 dpi ratios are 1 and ratios at other time points are relative to the 7 dpi ratio.

To dampen the excitability of adult-born GCs, we expressed a non-inwardly rectifying variant of the Kir2.1 potassium channel, Kir2.1 E224S (Yang et al., 1995), henceforth referred to as ESKir2.1. Expression of ESKir2.1 resulted in a leak current that reduced the cell's input resistance by ~ 2 fold and set a more negative resting membrane potential, thereby reducing the probability of neuronal spiking by increasing the requirement for synaptic input to achieve

firing threshold (Figure 1A-D). Expression of ESKir2.1 hyperpolarized the neuroblasts in the core of the OB as early as at 7 dpi (Figure S1A-H) and did not affect the initial stages of development of new GCs, as ESKir2.1$^+$ GCs successfully migrated into the OB and survived as well as control neurons up till 14 dpi (Figures 1E and S2C,D). This observation argues against the possibility that expression of this ion channel results in non-specific toxic effects in the new neurons.

Dampening electrical activity inhibits integration of adult-generated neurons into the OB

By 28 dpi, however, the number of ESKir2.1$^+$ neurons integrated into the OB was reduced by 57±8% (***; $p<0.002$; n = 4 bulbs; Figure 1E and S2E). Interestingly, this timing coincides with a critical period for integration of newly generated GCs in the postnatal OB, between 14 and 28 dpi, during which their survival is most sensitive to olfactory deprivation (Yamaguchi and Mori, 2005). These results demonstrate an important role of neuronal activity in regulating the integration of adult-generated neurons in a cell-autonomous manner. Interestingly, spine density and the frequency of spontaneous excitatory postsynaptic current (sEPSC) were indistinguishable between control and ESKir2.1$^+$ neurons, suggesting that suppression of cell-intrinsic neuronal activity has minimal effects on synaptic development (Figure S1I-L). However, the amplitude of sEPSC was higher for ESKir2.1$^+$ than controls neurons at 28 dpi (Figure S1J). This increase in sEPSC amplitude may reflect the synaptic scaling previously described in activity-deprived neurons (Turrigiano and Nelson, 2004).

Expression of the voltage-gated sodium channel NaChBac elevates electrical activity in adult-generated neurons

Recent studies propose that adult neurogenesis serves to facilitate experience-dependent modification of neural circuits for adaptation to environmental changes (Aimone et al., 2006; Wilbrecht et al., 2002). This hypothesis suggests that the timing of synaptic inputs relative to activity in the rest of the circuit, and their source and strength would all be predicted to participate in regulating the integration of new neurons. Alternatively, integration of new neurons may simply be determined by summing overall levels of activity in a neuron during a specific critical period, regardless of its source or timing, and neurons that meet a minimum threshold are retained. To investigate these possibilities, we increased neuronal activity in individual new GCs in the OB in a manner that reduces their dependency on synaptic input for firing, and evaluated the consequences of this manipulation on neuronal integration into the OB.

To disrupt normal firing patterns and increase the occurrence of neuronal firing, such that neuronal spiking would occur with synaptic inputs that are insufficient to evoke action potentials in control neurons, we used the bacterial voltage-gated sodium channel NaChBac. Two key properties of NaChBac allow for this: First, its activation threshold is approximately 15 mV more negative than that of native sodium channels in granule neurons (Kelsch et al., 2007); Second, it inactivates on the order of hundreds of milliseconds, compared to less than 1 ms in mammalian sodium channels (Bean, 2007; Ren et al., 2001). We have previously observed that NaChBac expression in GCs triggers depolarizations approximately 600 ms long (Kelsch et al., 2009). Such long depolarizations are not uncommon in neurons in the mammalian brain. For instance, cholinergic stimulation has been shown to trigger long depolarizations in several neuronal types (Fraser and MacVicar, 1996). Here we examined whether this phenomenon also occurs in newly generated GCs. Application of carbachol, a muscarinic agonist mimicking cholinergic input, induced long after-depolarization-potentials (ADPs) in adult-born GCs (Figure 2A). These long depolarizations robustly occurred in adult-born GCs during the early (18 dpi) but not late (28 dpi) phases of their integration into the OB (Figure 2A,B). The ADP triggered by carbachol was completely blocked by pre-applying atropine, a muscarinic receptor antagonist (Figures 2A and S2F-H). These findings suggest

that physiological stimuli, such as cholinergic innervation, can trigger long membrane depolarizations in adult-born GCs, similar to those induced by NaChBac expression.

We delivered NaChBac to GC precursors in the SVZ using the strategy described for ESKir2.1. To assess the ability of NaChBac to enhance the intrinsic excitability of new GCs, we performed whole cell patch clamp recordings between 14 to 16 dpi, at the beginning of their critical period for survival. At this stage, newly generated GCs expressing NaChBac-EGFP ($NaChBac^+$) have a slow inward current that activates at −41±1.8 mV, which causes neurons to fire spontaneous action potentials significantly more frequently than control neurons and with long plateau potentials lasting on average 608±68 ms (Figure 2D-F). In addition, we have observed that the electrophysiological effects of NaChBac expression on GCs persist throughout the duration of the critical period (Kelsch et al., 2009). Thus, NaChBac expression is sufficient to increase overall levels of neuronal activity in newly generated GCs.

Increased intrinsic electrical activity enhances the integration of adult-generated neurons into the OB

We assessed the effect of increasing electrical excitability via NaChBac expression on the integration of adult-born GCs into the OB, and found that up till 14 dpi, $NaChBac^+$ neurons migrated and integrated into the OB at similar levels to control neurons (Figure 2G and Figure S2A, B). However, beginning at 21 dpi, $NaChBac^+$ neurons integrated into the OB at significantly higher rates than control neurons (21 dpi: 22±6%; **P < 0.002; n = 4 bulbs; 28 dpi: 31±4%; ***p<0.0001; n = 10 bulbs; Figure 2G). This increase in survival persisted for as long as 2 months after infection (56 dpi; 25±3%; **p< 0.0001; n = 6 bulbs). Electrophysiological measurements of sEPSCs in $NaChBac^+$ neurons indicate that they received similar levels of excitatory synaptic input as compared to control neurons, demonstrating that the enhanced survival of $NaChBac^+$ neurons was accompanied by functional integration into the circuit (Figure 3A,B). Furthermore, $NaChBac^+$ neurons were morphologically similar to control neurons, with no changes in the pattern of dendritic arborization or in the linear density of synaptic spines (Figure 3C-G). This observation is consistent with our previous finding that NaChBac does not affect the density of clusters labeled with the synaptic marker PSD95-GFP in OB GCs (Kelsch et al., 2009). These observations illustrate that $NaChBac^+$ neurons are functional, and suggest that strong perturbations of cell-intrinsic neuronal activity via either NaChBac or ESKir2.1 expression have minimal effects on the synaptic development of these neurons.

Our findings suggest that increasing the overall intrinsic level of activity in an adult-born neuron is sufficient to confer a significant survival advantage to that cell, but do not allow us to specify whether adult-generated neurons normally have a requirement for patterns of synaptic input specifically driven by sensory experience in order to integrate into the bulb. Multiple studies have demonstrated that sensory input is crucial for the integration of new neurons into the OB (Alonso et al., 2006; Petreanu and Alvarez-Buylla, 2002), but it remains unclear whether sensory input simply provides a minimum, necessary level of synaptic drive onto new GCs to support survival, or if sensory-driven patterns of synaptic input contain information relevant to the selection of the new GC for integration.

NaChBac rescues adult-generated neurons from death in a sensory-deprived OB

To further explore these questions, we tested whether a NaChBac-mediated increase in neuronal activity can substitute for physiological sensory experience in mediating the integration of adult-born neurons into the OB. We co-injected a mixture of retroviruses bilaterally into the SVZ of animals in which we had unilaterally occluded one nostril, a procedure that eliminates sensory input to the ipsilateral bulb. Previous works have demonstrated that 50% of new neurons in the adult ultimately integrate into the normal OBs,

whereas nostril occlusion further reduces this proportion to 25% (Winner et al., 2002; Yamaguchi and Mori, 2005). The survival ratio of NaChBac$^+$ neurons compared to control cells in the non-occluded bulb was approximately 1.33, similar to that described above (Figure 2G,H); in contrast, in the occluded bulb this ratio was increased to approximately 1.76 (Figure 2H). Since olfactory deprivation results in approximately 50% decrease in the survival of new GCs, a complete rescue of sensory-dependent GC death by NaChBac in an occluded bulb would result in a survival ratio of 2; thus, a ratio of 1.76 indicates that NaChBac expression provides more than a 75% rescue of GC death resulting from sensory deprivation. This result demonstrates that increased neuronal excitability conferred by NaChBac expression is sufficient to partially substitute for the contribution of sensory-dependent synaptic input in regulating GC integration. This observation parallels our previous data showing that NaChBac expression blocks changes in synaptic density induced by sensory deprivation (Kelsch et al., 2009). Furthermore, this observation suggests that experience-driven synaptic input is not the only mechanism driving the selection of adult-born neurons for integration as corroborated by the finding that 25% of new neurons still survive in sensory deprived bulbs (Petreanu and Alvarez-Buylla, 2002; Yamaguchi and Mori, 2005).

NMDA receptor activity is essential for integration of adult-generated neurons in the OB

Because NaChBac promotes neuronal integration independent of experience-driven synaptic input, it is probable that the mechanism regulating activity-dependent survival is directly tracking the levels of membrane depolarization. The membrane potential of a neuron is constantly modulated by neurotransmitters acting on synaptic receptors, and in the central nervous system, AMPA- and NMDA-receptors (NMDARs) are the major receptors mediating membrane depolarization. Previous studies have suggested that NMDAR activity regulates the survival of adult-born neurons in the dentate gyrus (Tashiro et al., 2006a). The requirement of NMDAR signaling for neuronal survival may depend on the detection of coincident pre- and post-synaptic activity, such as in spike-timing dependent plasticity (Dan and Poo, 2006), or alternatively, the requirement of NMDAR function for new neuron survival may simply reflect the contribution of NMDAR activity to overall levels of neuronal depolarization in new GCs.

To investigate the contribution of NMDAR to new neuron integration, we first sought to confirm the requirement for NMDAR function in the survival of new GCs in the OB. We genetically ablated the essential NR1 subunit to eliminate all NMDAR-mediated input in individual new GCs by sparsely infecting progenitor cells in the SVZ of *NR1* floxed conditional mice (*NR1*$^{fl/fl}$) with retroviral vectors encoding the Cre recombinase enzyme (Kohara et al., 2007; Tashiro et al., 2006b). Cre-mediated ablation of *NR1* successfully eliminated NMDAR expression since application of NMDA failed to induce any currents in Cre$^+$ neurons in *NR1*$^{fl/fl}$ mice (Figure 4A-C). By 28 dpi, virtually all NMDAR-deficient neurons were eliminated (Figure 4D,E). In comparison, no change in the survival of EGFP-CRE$^+$ neurons was observed in *NR1*$^{+/+}$ littermates (Figure 4D). This result demonstrates that the NMDAR, whose ablation decreases the survival of new dentate gyrus neurons by only 50% (Tashiro et al., 2006a), is absolutely required for the integration of adult-born GCs in the OB.

NaChBac expression rescues NMDAR-deficient adult-generated neurons from death

We next determined whether increasing activity in new GCs via NaChBac expression could substitute for NMDAR function in supporting neuronal integration into the OB. NaChBac and Cre recombinase were simultaneously delivered into *NR1*$^{fl/fl}$ mice, and GC integration was assessed. We found that increasing the excitability of newly generated NMDAR-deficient GCs via NaChBac expression completely rescued their death (Figure 4D,E). The dendritic morphology of NaChBac$^+$ NMDAR-deficient neurons appeared similar to that of control neurons and received AMPAR-mediated synaptic input (Figure S3), indicating that they functionally integrated into the bulb's circuit. These results demonstrate that the requirement

for NMDARs in the integration of new GCs most likely reflects the contribution of NMDARs to the overall levels of neuronal activity in the neuron. Furthermore, our data support a model in which activity-dependent integration depends on overall levels of membrane depolarization, irrespective of how this depolarization is achieved.

DISCUSSION

An activity threshold for integration of new adult-born neurons into the OB circuit

To elucidate whether synaptic input regulates survival by providing new neurons with a precise pattern of neuronal activity, or merely a minimal level of membrane depolarization, we used NaChBac, a bacterial voltage-gated sodium channel, to perturb the spiking pattern of new neurons while simultaneously elevating their activity levels. Our results indicate that the integration of new neurons into the OB circuit predominantly depends on their overall levels of membrane depolarization, regardless of the pattern of action potentials generated. Interestingly, tonic cholinergic stimulation, which causes sustained depolarizations in adult-born OB neurons during their early integration (Figures 2A-C and S2), has recently been shown to enhance the survival of new neurons both in the OB and dentate gyrus (Kaneko et al., 2006). Conversely, the removal of cholinergic input into the OB compromises the survival of new neurons (Cooper-Kuhn et al., 2004). Given our findings about depolarization-enhanced integration, the long depolarizations induced by cholinergic stimulation may directly contribute to the improved survival of new neurons observed in previous studies (Kaneko et al., 2006). Interestingly, the long depolarizations induced by cholinergic stimulation occur robustly in young GCs during the critical period of survival at 18 dpi but not after maturation at 28 dpi, indicating a possible role of prolonged cholinergic-induced depolarization specifically in driving survival of new OB granule neurons. General behavioral states, such as running, stress, attentiveness and depression affect neuronal integration of new neurons into adult brains (Gould et al., 1997;Malberg et al., 2000;Mouret et al., 2008;van Praag et al., 1999). Our results suggest that neuromodulators such as acetylcholine may mediate these effects by acting as significant regulators of the level of depolarization of new neurons.

The notion that general membrane depolarization is a determinant of neuronal integration is further supported by our observation that although NMDAR expression is essential for new neuron integration, NaChBac-mediated depolarization is sufficient to fully rescue NMDAR-deficient neurons from death. Hence, the requirement of NMDAR in new neuron survival may be due to the extended depolarization caused by its slow gating kinetics. Interestingly, recent evidence also indicates that the contribution of NMDAR for synaptic vesicle release in GCs is not directly through the calcium entry through its pore but indirectly through the influx of calcium through voltage-gated calcium channels, which open as a result of the long depolarization induced by NMDAR activity (Isaacson, 2001; Schoppa et al., 1998). Together, our data support a model in which activity-dependent integration depends on overall levels of membrane depolarization, determined, for instance, by monitoring calcium influx through L-type voltage-gated calcium channels (Dolmetsch et al., 2001), rather than specifically on neuronal activity mediated by postsynaptic glutamate receptors.

It is not yet known how activity levels could be monitored in order to determine if a particular cell achieves the minimum threshold of neuronal activity required to survive and successfully integrate into the adult brain. New adult-born neurons could act as integrators that measure and summate levels of activity over a critical period, lasting perhaps on the time scale of days, to compute this life or death decision (McCormick, 2001). This critical period spans a time period sometime between 14 to 28 days after the birth of the neuron, when sensory deprivation or ESKir2.1-mediated suppression of activity has the strongest effect on survival (Yamaguchi and Mori, 2005). Alternatively, instantaneous levels of activity may be continuously evaluated

such that neurons that never meet the minimum threshold of activity during the critical period are eliminated.

Determinants of dendritic morphology of GCs in the OB

When we introduced ESKir2.1 into GCs in the OB, we observed that although the electrical properties of these neurons were altered significantly, their dendritic structures remained unchanged. This is unexpected because overexpression of Kir2.1 in neurons has been previously shown to alter the morphology of axons, in transfected retinal neurons in zebrafish (Hua and Smith, 2004), as well as dendrites, in transfected rat hippocampal neurons *in vitro* (Burrone et al., 2002). Two non-mutually exclusive explanations could account for our findings. First, in previous experiments, Kir2.1 channels were expressed in excitatory neurons (Burrone et al., 2002; Hua and Smith, 2004), whereas here we specifically target inhibitory interneurons. The plasticity responses of excitatory and inhibitory neurons differ in many respects (Bi and Poo, 1998), and it is plausible that electrical silencing by Kir2.1 channels affects the morphology of excitatory, but not inhibitory neurons. Next, gene delivery methods used in previous work induce much higher levels of Kir2.1 expression than what we report here with oncoretroviral delivery. For instance, calcium-phosphate transfection of Kir2.1 into cultured hippocampal neurons lowers the neurons' input resistance from 166+/−11 to 63+/−25 MΩ, which corresponds to a 10,000 pS increase of Kir2.1 conductance (Burrone et al., 2002). In contrast, our oncoretroviral vector delivery of ESkir2.1 results in expression levels that only introduces 600 pS of resting leak conductance and lowers the input resistance of GCs from 1147+/−59 to 655+/−76 MΩ, even though neuronal firing is largely eliminated. Thus, it is possible that the changes in neuronal morphology previously reported were not solely due to reduction of neuronal excitability by Kir2.1 activity, but to additional effects resulting from very high levels of expression.

Reduction of sensory input by olfactory deprivation has been shown to modify synaptic structure of GCs (Saghatelyan et al., 2005). We have recently confirmed this observation using genetic labeling of postsynaptic glutamatergic densities with the PSD95-GFP marker (Kelsch et al., 2009). In addition, we observed that whereas NaChBac did not affect the density of PSD95-GFP synapses in normal conditions, it blocked the synaptic changes triggered by olfactory deprivation (Kelsch et al., 2009). These observations suggest an interaction between sensory input and intrinsic membrane excitability to achieve a minimal level of neuronal activity necessary for the normal development of synapses in GCs. Our current results indicate that this principle also extends to neuronal survival, since there seems to be a minimum threshold of neuronal activity required for the integration of young GCs into the OB. This threshold level of activity can similarly be provided by a combination of synaptic input and intrinsic membrane excitability. Our experiments indicate that the elevation of intrinsic excitability via NaChBac expression is sufficient to counteract the reduction of sensory input. Reaching this minimal level of activity both rescues young GCs from death and allows them to acquire normal synaptic organization in an odor-deprived OB.

Determinants of overall activity level in new neurons

What drives overall activity levels, and hence survival of new adult-born neurons during the critical period? One feature of the critical period is that it coincides with the onset of synapse formation in GCs, and this has led previous studies to primarily focus on the role of phasic synaptic input, as regulated by sensory experience, in new neuron survival. In addition, during this critical period the intrinsic conductance (e.g. A-type potassium channels, voltage-gated sodium channels) of new neurons undergo major changes as the neurons mature. Our findings show that in addition to synaptic input, membrane conductance, as determined by the repertoire of ion channels expressed by new neurons, may play a pivotal role in regulating integration and survival. Variability in membrane conductance between neurons of the same type has been

shown to be significant (Marder and Goaillard, 2006), and fluctuations in the intrinsic excitability of young neurons could result in differing levels of synaptic input required for their survival. In addition, the intrinsic excitability of OB neurons is strongly modulated by centrifugal innervation originating from other parts of the brain. In particular, cholinergic stimulation induces long-lasting depolarizations in GCs, which facilitate persisting firing modes (Figure S2 and Pressler et al 2007). These phenomena could account for the observation that cells rendered hyperexcitable by NaChBac expression are able to survive with reduced levels of synaptic input resulting from olfactory deprivation or NMDAR ablation. In this manner, the overall level of activity, as determined by the combination of synaptic inputs received and intrinsic membrane properties, drives integration of new neurons into a circuit.

EXPERIMENTAL PROCEDURES

Retroviral vectors

Cloning of the viral constructs encoding ESKir2.1, NaChBac and Cre was performed using standard molecular techniques. Production and titration of retroviral particles were performed as previously described (Kelsch et al., 2007). See Supplemental Experimental Procedures for details.

Retroviral labeling *in vivo*

Retroviral vectors were stereotaxically injected into the SVZ of adult rats and mice as previously described, with slight modification (Kelsch et al., 2008; Kelsch et al., 2007). See Supplemental Experimental Procedures for details.

Histology and morphological analysis

Rats and mice injected with retroviruses were anesthesized, intracardially perfused and their olfactory bulbs processed for histology and morphological analysis as previously described (Kelsch et al., 2008; Kelsch et al., 2007). See Supplemental Experimental Procedures for details.

Olfactory deprivation

Unilateral olfactory deprivation was performed by unilaterally electrocauterizing one nostril of deeply anesthetized rats immediately after viral injection. See Supplemental Experimental Procedures for details.

Survival ratio analysis

Two viruses were mixed at an approximate 1:1 ratio for survival analysis. One of the viruses carried the construct encoding mCherry, while the other carried one of a range of constructs: hrGFP linked to ESKir2.1 by an EMC IRES, EGFP alone, NaChBac or NaChBac E191K fused to EGFP (NaChBac-EGFP or NaChBacE191K-EGFP), and Cre Recombinase linked with the 2A linker to EGFP, NaChBac-EGFP or NaChBacE191K-EGFP (NaChBac-Cre or NaChBacE191K-Cre). Fluorescently labeled cells were quantified with the aid of the Neurolucida software (MicroBright Field Inc.). The survival ratio is defined as the total number of EGFP-positive cells (including double-labeled cells) divided by of the number of singly labeled mCherry-expressing cells. The ratio of $EGFP^+$ to $mCherry^+$ neurons at 7 days post infection (dpi) was used to normalize all data at subsequent time points for comparison, hence ratios at all subsequent time points were relative to the 7 dpi ratio. Three to 7 entire sections per olfactory bulb were analyzed to collect at least 400 counted cells in each bulb. The mean survival ratio from each bulb was treated as a single sample.

Electrophysiological recordings and analysis

Whole-cell patch-clamp recordings of fluorescently labeled neurons in acute slices were performed and analyzed as described previously (Kelsch et al., 2009; Kelsch et al., 2007). See Supplemental Experimental Procedures for details.

Statistical analysis

The Mann-Whitney test was used for comparing the frequency of spontaneous firing in $NaChBac^{+}$ and control neurons at resting membrane potential to determine statistical significance (Figure 2C). To analyze survival rates in sensory-deprived versus control bulbs, the paired Student's *t*-test was used since these were paired bulbs of the same animal (Figure 2E). All other data was analyzed with the two-sample two-tailed Student's *t*-test in OriginPro 8 (Origin Lab Corporation). Data was reported as mean ± SEM.

Supplementary Material

Refer to Web version on PubMed Central for supplementary material.

Acknowledgments

We thank Alberto Stolfi and Drew Friedman for help with engineering of the viral constructs, David Clapham for providing us with NaChBac cDNA, Susumu Tonegawa for providing conditional NR1 mice, Benjamin Scott for help with two-photon imaging, and Leopoldo Petreanu, Sacha Nelson, Suzanne Paradis and Elizabeth Hong for comments on the manuscript. This work was supported by an NIDCD RO1 grant to C.L., an M.I.T. Singleton and Chyn Duog Shiah Memorial fellowships to C.W.L., and a Newton postdoctoral fellowship to W.K.

REFERENCES

Aimone JB, Wiles J, Gage FH. Potential role for adult neurogenesis in the encoding of time in new memories. Nat Neurosci 2006;9:723–727. [PubMed: 16732202]

Alonso M, Viollet C, Gabellec MM, Meas-Yedid V, Olivo-Marin JC, Lledo PM. Olfactory discrimination learning increases the survival of adult-born neurons in the olfactory bulb. J Neurosci 2006;26:10508–10513. [PubMed: 17035535]

Bean BP. The action potential in mammalian central neurons. Nat Rev Neurosci 2007;8:451–465. [PubMed: 17514198]

Bi GQ, Poo MM. Synaptic modifications in cultured hippocampal neurons: dependence on spike timing, synaptic strength, and postsynaptic cell type. J Neurosci 1998;18:10464–10472. [PubMed: 9852584]

Burrone J, O'Byrne M, Murthy VN. Multiple forms of synaptic plasticity triggered by selective suppression of activity in individual neurons. Nature 2002;420:414–418. [PubMed: 12459783]

Buss RR, Sun W, Oppenheim RW. Adaptive roles of programmed cell death during nervous system development. Annu Rev Neurosci 2006;29:1–35. [PubMed: 16776578]

Cooper-Kuhn CM, Winkler J, Kuhn HG. Decreased neurogenesis after cholinergic forebrain lesion in the adult rat. J Neurosci Res 2004;77:155–165. [PubMed: 15211583]

Dan Y, Poo MM. Spike timing-dependent plasticity: from synapse to perception. Physiol Rev 2006;86:1033–1048. [PubMed: 16816145]

Dolmetsch RE, Pajvani U, Fife K, Spotts JM, Greenberg ME. Signaling to the nucleus by an L-type calcium channel-calmodulin complex through the MAP kinase pathway. Science 2001;294:333–339. [PubMed: 11598293]

Fraser DD, MacVicar BA. Cholinergic-dependent plateau potential in hippocampal CA1 pyramidal neurons. J Neurosci 1996;16:4113–4128. [PubMed: 8753873]

Gould E, McEwen BS, Tanapat P, Galea LA, Fuchs E. Neurogenesis in the dentate gyrus of the adult tree shrew is regulated by psychosocial stress and NMDA receptor activation. J Neurosci 1997;17:2492–2498. [PubMed: 9065509]

Hua JY, Smith SJ. Neural activity and the dynamics of central nervous system development. Nat Neurosci 2004;7:327–332. [PubMed: 15048120]

Isaacson JS. Mechanisms governing dendritic gamma-aminobutyric acid (GABA) release in the rat olfactory bulb. Proc Natl Acad Sci U S A 2001;98:337–342. [PubMed: 11120892]

Kaneko N, Okano H, Sawamoto K. Role of the cholinergic system in regulating survival of newborn neurons in the adult mouse dentate gyrus and olfactory bulb. Genes Cells 2006;11:1145–1159. [PubMed: 16999735]

Kee N, Teixeira CM, Wang AH, Frankland PW. Preferential incorporation of adult-generated granule cells into spatial memory networks in the dentate gyrus. Nat Neurosci 2007;10:355–362. [PubMed: 17277773]

Kelsch W, Lin CW, Lois C. Sequential development of synapses in dendritic domains during adult neurogenesis. Proc Natl Acad Sci U S A 2008;105:16803–16808. [PubMed: 18922783]

Kelsch W, Lin CW, Mosley CP, Lois C. A critical period for activity-dependent synaptic development during olfactory bulb adult neurogenesis. J Neurosci 2009;29:11852–11858. [PubMed: 19776271]

Kelsch W, Mosley CP, Lin CW, Lois C. Distinct mammalian precursors are committed to generate neurons with defined dendritic projection patterns. PLoS Biol 2007;5:e300. [PubMed: 18001150]

Kohara K, Yasuda H, Huang Y, Adachi N, Sohya K, Tsumoto T. A local reduction in cortical GABAergic synapses after a loss of endogenous brain-derived neurotrophic factor, as revealed by single-cell gene knock-out method. J Neurosci 2007;27:7234–7244. [PubMed: 17611276]

Lledo PM, Alonso M, Grubb MS. Adult neurogenesis and functional plasticity in neuronal circuits. Nat Rev Neurosci 2006;7:179–193. [PubMed: 16495940]

Lois C, Alvarez-Buylla A. Long-distance neuronal migration in the adult mammalian brain. Science 1994;264:1145–1148. [PubMed: 8178174]

Malberg JE, Eisch AJ, Nestler EJ, Duman RS. Chronic antidepressant treatment increases neurogenesis in adult rat hippocampus. J Neurosci 2000;20:9104–9110. [PubMed: 11124987]

Marder E, Goaillard JM. Variability, compensation and homeostasis in neuron and network function. Nat Rev Neurosci 2006;7:563–574. [PubMed: 16791145]

McCormick DA. Brain calculus: neural integration and persistent activity. Nat Neurosci 2001;4:113–114. [PubMed: 11175863]

Mouret A, Gheusi G, Gabellec MM, de Chaumont F, Olivo-Marin JC, Lledo PM. Learning and survival of newly generated neurons: when time matters. J Neurosci 2008;28:11511–11516. [PubMed: 18987187]

Petreanu L, Alvarez-Buylla A. Maturation and death of adult-born olfactory bulb granule neurons: role of olfaction. J Neurosci 2002;22:6106–6113. [PubMed: 12122071]

Ren D, Navarro B, Xu H, Yue L, Shi Q, Clapham DE. A prokaryotic voltage-gated sodium channel. Science 2001;294:2372–2375. [PubMed: 11743207]

Saghatelyan A, Roux P, Migliore M, Rochefort C, Desmaisons D, Charneau P, Shepherd GM, Lledo PM. Activity-dependent adjustments of the inhibitory network in the olfactory bulb following early postnatal deprivation. Neuron 2005;46:103–116. [PubMed: 15820697]

Schoppa NE, Kinzie JM, Sahara Y, Segerson TP, Westbrook GL. Dendrodendritic inhibition in the olfactory bulb is driven by NMDA receptors. J Neurosci 1998;18:6790–6802. [PubMed: 9712650]

Tashiro A, Sandler VM, Toni N, Zhao C, Gage FH. NMDA-receptor-mediated, cell-specific integration of new neurons in adult dentate gyrus. Nature 2006a;442:929–933. [PubMed: 16906136]

Tashiro A, Zhao C, Gage FH. Retrovirus-mediated single-cell gene knockout technique in adult newborn neurons in vivo. Nat Protoc 2006b;1:3049–3055. [PubMed: 17406567]

Turrigiano GG, Nelson SB. Homeostatic plasticity in the developing nervous system. Nat Rev Neurosci 2004;5:97–107. [PubMed: 14735113]

van Praag H, Kempermann G, Gage FH. Running increases cell proliferation and neurogenesis in the adult mouse dentate gyrus. Nat Neurosci 1999;2:266–270. [PubMed: 10195220]

Wilbrecht L, Crionas A, Nottebohm F. Experience affects recruitment of new neurons but not adult neuron number. J Neurosci 2002;22:825–831. [PubMed: 11826112]

Winner B, Cooper-Kuhn CM, Aigner R, Winkler J, Kuhn HG. Long-term survival and cell death of newly generated neurons in the adult rat olfactory bulb. Eur J Neurosci 2002;16:1681–1689. [PubMed: 12431220]

Yamaguchi M, Mori K. Critical period for sensory experience-dependent survival of newly generated granule cells in the adult mouse olfactory bulb. Proc Natl Acad Sci U S A 2005;102:9697–9702. [PubMed: 15976032]

Yang J, Jan YN, Jan LY. Control of rectification and permeation by residues in two distinct domains in an inward rectifier K+ channel. Neuron 1995;14:1047–1054. [PubMed: 7748552]

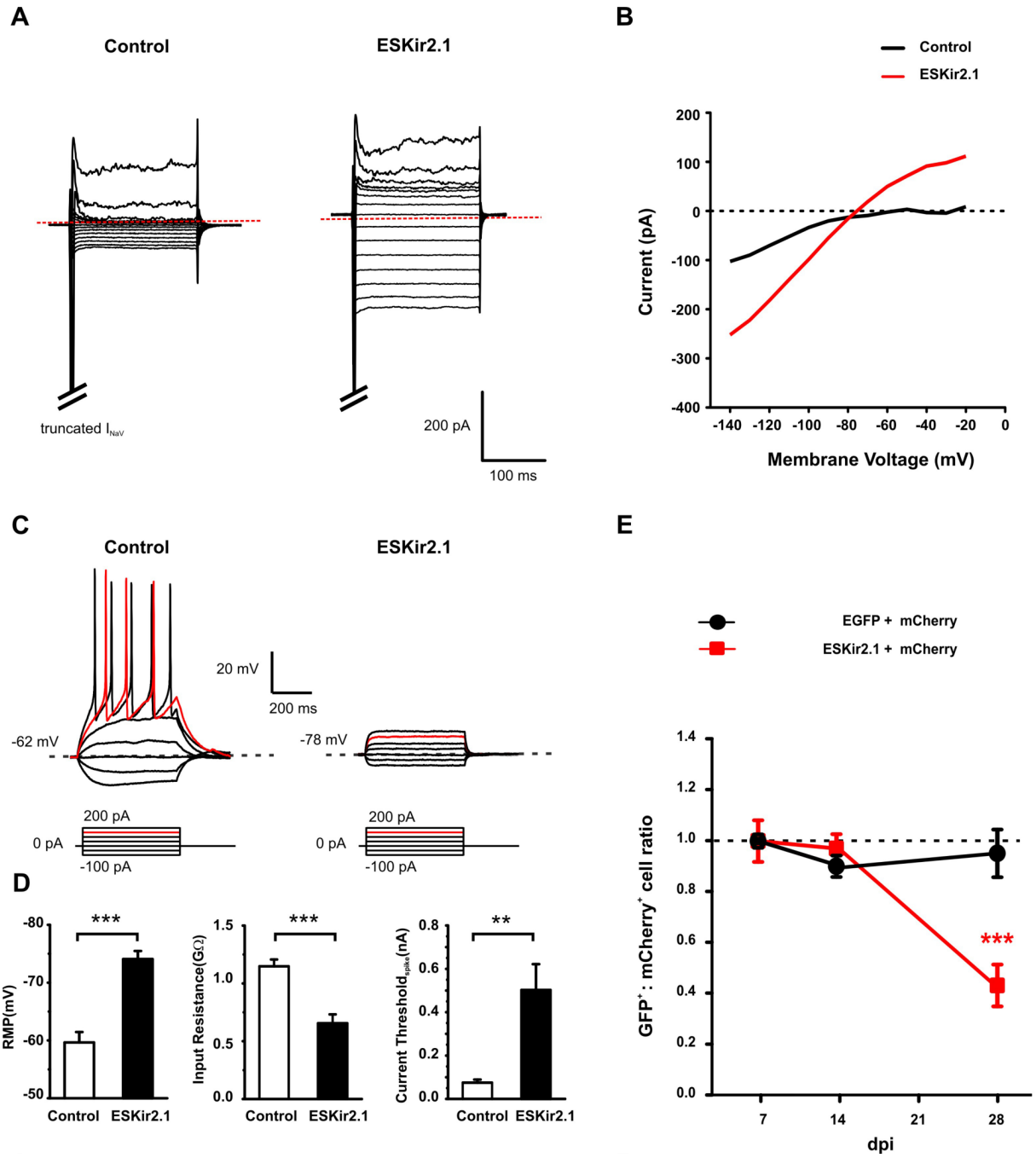

Figure 1. Decreased intrinsic neuronal activity via ESKir2.1 expression compromises the survival and integration of adult-generated neurons

(A) Current-voltage relationship in control (mCherry$^+$) and ESKir2.1$^+$ neurons. Neurons were clamped at −70 mV and stepwise voltage was applied from −140 to 0 mV.

(B) ESKir2.1$^+$ neurons displayed larger steady-state leak currents than control neurons.

(C) The amount of current sufficient to trigger action potentials in control neurons (left) was below the threshold necessary to elicit action potentials in new neurons expressing ESKir2.1 (right).

(D) Relative to control neurons at 16-18 dpi, ESKir2.1 expression hyperpolarized neurons by 14±2.4 mV (left, ***$p < 0.000003$; n = 13 neurons), decreased their input resistance by 492

±100.3 MΩ (center, ***$p < 0.0002$; $n = 11$ neurons), and increased the minimal amount of current required to reach spiking threshold by 0.427±0.13 nA (right, **$p < 0.004$; $n = 10$ neurons).

(E) Normalized survival ratios (Number of $EGFP^+$ cells, including double-labeled cells, divided by the number of singly labeled $mCherry^+$ cells, normalized to the 7 dpi value) of ESKir2.1/$hrGFP^+$ and $EGFP^+$ neurons. By 28 dpi, ESKir2.1$^+$ neurons survived significantly less well than control neurons (red line; −56±12%; $n = 4$ bulbs each group; **$p < 0.002$) while EGFP did not have an effect (black line; $p < 0.636$; $n = 4$ bulbs).

Two-tailed t-test used for statistical analysis. Error bars represent SEM.

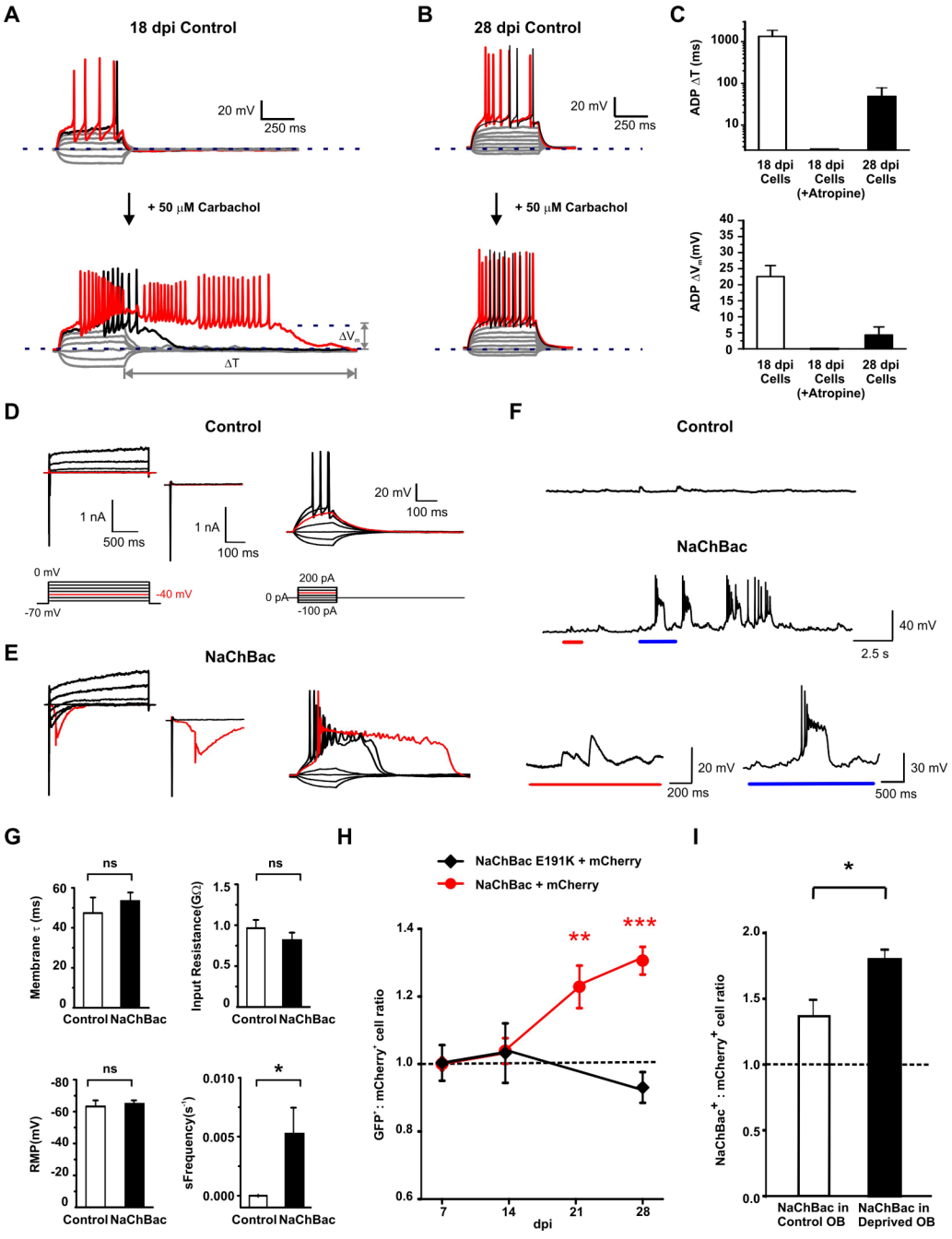

Figure 2. Increased intrinsic neuronal activity via NaChBac expression enhances the survival of adult-generated neurons

(A) Carbachol induced a long-lasting after-depolarization-potential (ADP) in 18 dpi GCs. Additionally, carbachol increased spike numbers upon suprathreshold stimulation.

(B) Carbachol enhanced membrane excitability of 28 dpi GCs by increasing spike numbers upon suprathreshold stimulation, but did not induce the long ADP observed at 18 dpi.

(C) (Upper panel) The after-depolarization-potential (ADP) induced by carbachol was much longer in 18 dpi than in 28 dpi neurons. (Lower panel) The amplitude of ADP induced by carbachol was significantly larger in 18 dpi than in 28 dpi neurons.

(D) (Upper left and center) At 18 dpi, new control neurons (mCherry$^+$) recorded in voltage-clamp mode displayed > 2 nA of voltage-sensitive sodium inward current at −10 mV, but none at −40 mV (red trace). In contrast, NaChBac$^+$ neurons (red trace, lower left and center) had a 762±119 pA slow inward current opening at −43±2.1 mV (n = 6 neurons) and >2 nA of inward current at −20 mV. In current-clamp mode (right), a 200 ms pulse of positive 150 pA current injection generated repetitive action potentials in control neurons (upper right) whereas repetitive action potentials with sustained depolarization (608±68 ms, n = 6 neurons) were induced in NaChBac$^+$ neurons (red trace, lower right).

(E) In current-clamp mode, control neurons (top trace) did not fire action potentials, while NaChBac expression resulted in spontaneous, repetitive firing at resting membrane potential (middle trace). A closer look at the NaChBac trace (bottom left) shows that NaChBac$^+$ neurons received functional synaptic inputs as indicated by frequent spontaneous synaptic events. These neurons fired action potentials mediated by endogenous sodium channels riding atop NaChBac-mediated depolarization (bottom right).

(F) All passive electrical properties in NaChBac$^+$ neurons remained similar to control neurons except for a significantly higher rate of spontaneous firing (NaChBac, 0.02±0.007 Hz; Control, 0.004±0.004 Hz; *p <0.01; Mann-Whitney test; n = 6 neurons in each group).

(G) Cell survival ratios of neurons with increased intrinsic excitability. NaChBac$^+$ neurons survived significantly better than control neurons at 21 dpi (red line; 22±6%; *n* = 4 bulbs; **p < 0.001) and 28 dpi (31±4%; n = 10 bulbs; ***p < 0.0001). The non-conducting mutant NaChBac E191K (black line) did not alter survival.

(H) NaChBac increased the relative survival of adult-generated neurons by a significantly larger factor in the sensory-deprived compared to the non-deprived OB (42±14%; *p <0.05; n = 4 deprived bulbs, n = 4 control bulbs; paired sample t-test).

Two-tailed t-test used for statistical analysis. Error bars represent SEM.

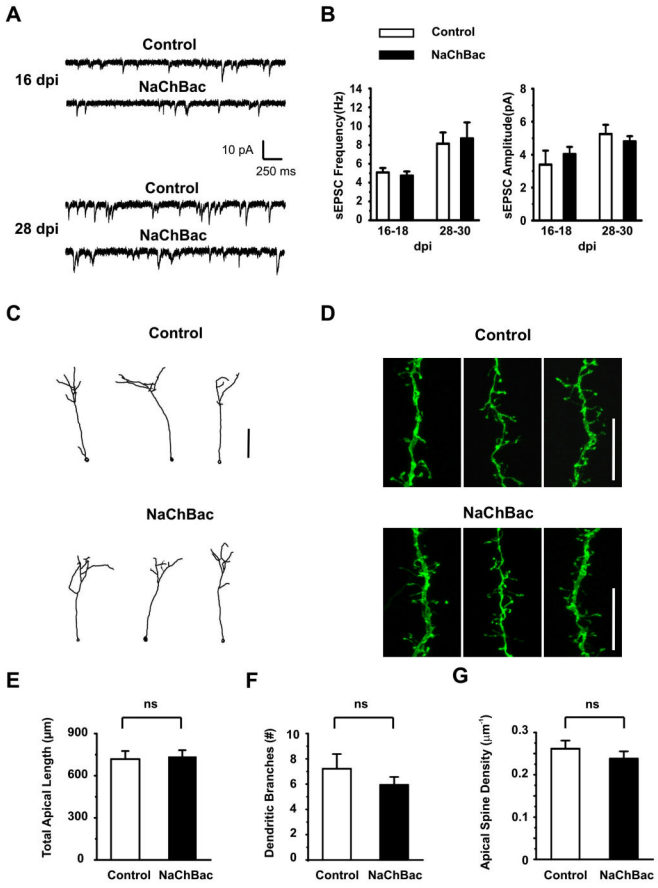

Figure 3. NaChBac$^+$ neurons receive normal synaptic input and display identical morphological characteristics as wild-type neurons

(A) Spontaneous excitatory postsynaptic current (sEPSC) was recorded in NaChBac$^+$ or mCherry$^+$ neurons at 16 and 28 dpi.

(B) NaChBac$^+$ neurons had similar sEPSC frequency and amplitude to control neurons in both the early (16-18 dpi) and late phase (28-30 dpi) of the critical period for survival.

(C) 3-dimensional Neurolucida reconstructions of representative granule neurons. Scale bar represents 100 μm.

(D) Confocal images showing representative dendrite sections. Scale bar represents 20 μm.

(E-G) NaChBac$^+$ neurons in the OB did not display altered apical length ($p < 0.78$; n = 20-25 neurons per group) (C), dendritic branching ($p < 0.39$; n = 14-16 neurons per group) (D) or apical spine density ($p < 0.33$; n = 8-10 neurons per group) (E).

Two-tailed t-test used for statistical analysis. Error bars represent SEM.

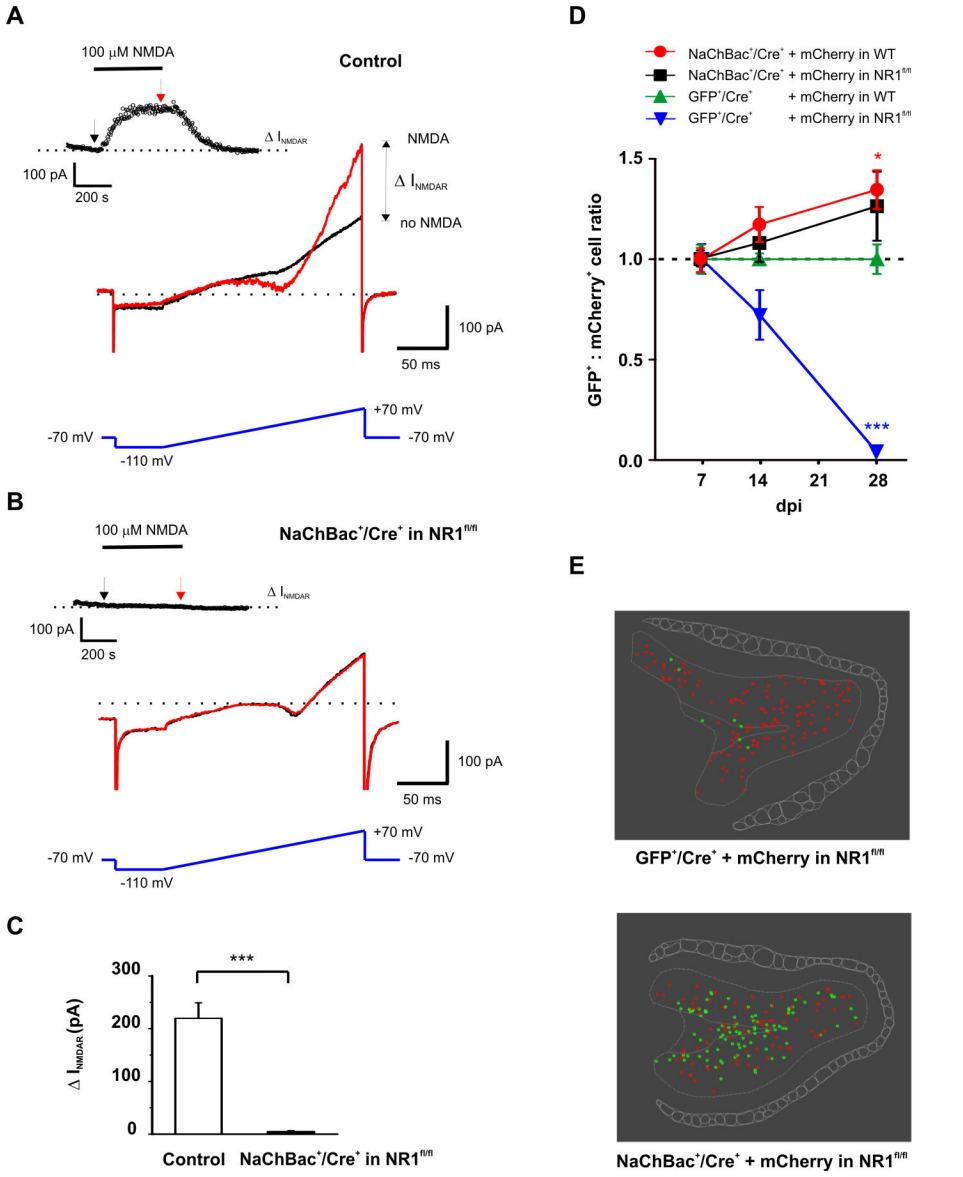

Figure 4. Increased intrinsic neuronal activity protects NMDAR-deficient neurons from death

(A) Application of 100 μM NMDA activated NMDAR-mediated currents measured at +70 mV in a single control neuron (mCherry^{+}) at 18 dpi (inset). The voltage ramp protocol, from −110 to +70 mV, performed before (black arrow) and during NMDA application (red arrow) showed characteristics of outward-rectifying NMDA currents (red trace) evoked by 1 mM Mg^{2+} present in bath solution.

(B) Expression of the NaChBac-Cre construct completely eliminated NMDAR-mediated currents as examined by application of 100 μM NMDA (inset). The I-V curve remained unchanged before (black trace) and after (red trace) NMDA application.

(C) 100 μM NMDA application elicited 220±29 pA NMDAR-mediated current in 18 dpi control neurons but none in neurons expressing the NaChBac-Cre construct (n = 4 neurons in each group).

(D) Survival rates of control (EGFP/Cre in WT), NR1$^{-/-}$ (EGFP/Cre in NR1$^{fl/fl}$), NaChBac^{+} (NaChBac/Cre in WT) and NR1$^{-/-}$ NaChBac^{+} neurons (NaChBac/Cre in NR1$^{fl/fl}$) in the OB. As expected, NaChBac^{+} neurons survived significantly better than control at 28 dpi in wild-

type OBs (red circles; 34.64±12.17%; *p <0.05; n = 5 bulbs). NMDAR-deficient neurons were completely eliminated by 28 dpi (blue triangles; −96.3±0.1%; ***p <0.0001; n = 3 bulbs) but survived as well as control neurons when they expressed NaChBac (black squares; p <0.1290; n = 5 bulbs).

(E) Neurolucida trace images showing representative distributions of $EGFP^+$ and $mCherry^+$ cells within representative OB sections at 28dpi.

Two-tailed t-test used for statistical analysis. Error bars represent SEM.